View metadata, citation and similar papers at core.ac.uk

brought to you by CORE

provided by VU Research Portal

VU UNIVERSITEIT AMSTERDAM

VU Research Portal

Stark manifolds and electric-field-induced avoided level crossings in helium Rydberg states

Lahaye, C.T.W.; Hogervorst, W.

published in
Physical Review A. Atomic, Molecular and Optical Physics
1989

DOI (link to publisher)
10.1103/PhysRevA.39.5658

document version
Publisher's PDF, also known as Version of record

Link to publication in VU Research Portal

citation for published version (APA)
Lahaye, C. T. W., & Hogervorst, W. (1989). Stark manifolds and electric-field-induced avoided level crossings in helium Rydberg states. *Physical Review A. Atomic, Molecular and Optical Physics*, *39*(11), 5658-5665. https://doi.org/10.1103/PhysRevA.39.5658

General rights
Copyright and moral rights for the publications made accessible in the public portal are retained by the authors and/or other copyright owners and it is a condition of accessing publications that users recognise and abide by the legal requirements associated with these rights.

- Users may download and print one copy of any publication from the public portal for the purpose of private study or research.
- You may not further distribute the material or use it for any profit-making activity or commercial gain
- You may freely distribute the URL identifying the publication in the public portal ?

Take down policy
If you believe that this document breaches copyright please contact us providing details, and we will remove access to the work immediately and investigate your claim.

E-mail address:
vuresearchportal.ub@vu.nl

Download date: 23. May. 2021

Stark manifolds and electric-field-induced avoided level crossings in helium Rydberg states

C. T. W. Lahaye and W. Hogervorst
Faculteit Natuurkunde en Sterrenkunde, Vrije Universiteit, De Boelelaan 1081, 1081 HV Amsterdam, The Netherlands
(Received 28 November 1988)

The linear Stark effect in $1snp\ ^{1,3}P$ Rydberg states ($n \approx 40$) of the fundamental two-electron atom helium was studied with the resolution of cw laser spectroscopy. The evolution of the angular-momentum manifolds was followed up to the regime where Stark states originating from different n values interact. Narrow avoided level crossings were detected with high precision. Stark manifolds were also calculated by diagonalization of the complete energy matrix in the presence of an electric field. In these calculations, even at moderate values of the field up to five n values have to be included to accurately reproduce the experimental data.

I. INTRODUCTION

In recent experiments in our laboratory, fine and hyperfine structure in the $1snp$ Rydberg series of ^{3}He and ^{4}He up to high values of the principal quantum number ($n \approx 80$) as well as isotope shifts were measured.[1,2] This work is part of a program to study in detail the properties of bound Rydberg and autoionizing levels of two-electron atoms,[2-5] where the electron-electron interaction manifests itself most clearly.[6,7] This program also includes an investigation of the influence of external fields, which may provide important additional information on the level structure of these atoms. Measurement of electric-dipole polarizabilities (quadratic Stark effect), for example, not only yields information on energies and wave functions of the levels in question, but also, via the coupling by the electric field, on those of the nearby opposite-parity levels.[8] Also high-angular-momentum levels, not directly accessible from atomic ground states or low-lying metastable states, may be populated in the presence of an electric field (linear Stark effect).[9]

The helium atom is the simplest, fundamentally most interesting two-electron system for which highly accurate calculations are available.[10] A review of calculations and experimental results on energies and fine-structure intervals of low-lying n states ($n < 9$) is given by Martin.[11] To further test the calculations there is a need for accurate data on high n states, for which information is scarce,[1] and for more accurate experimental results on low-lying states.[11] Information on the Stark effect in helium is also scarce. Values for the tensor polarizabilities of the $1snd\ ^{1,3}D$ series up to $n=7$ (Refs. 12–14) and for the $1s4f\ ^1F_3$ and $1s5f\ ^1F_3$ levels[15] have been reported recently.

This lack of accurate data on the bound $1snl$ Rydberg levels of helium may be attributed to the experimental difficulty of populating these levels, which lie almost 200 000 cm^{-1} above the $1s^2\ ^1S_0$ ground state. The development of an effective source of metastable $1s2s\ ^1S_0, ^3S_1$ atoms in conjunction with the production of tunable, narrow-band cw laser radiation in the wavelength region 260–335 nm in our laboratory created a facility to study in high resolution the $1snp\ ^{1,3}P$ Rydberg series of ^{3}He and ^{4}He. As an extension of our previous work[1,2] here the first results on linear Stark effect studies in the $1snp\ ^{1,3}P$ Rydberg levels of ^{4}He with $n \approx 40$ are reported. A study of helium is also of interest as all zero-field parameters, which have to be used for calculations of the Stark effect, are known with high precision.[11]

The quantum defects of the ^1P and ^3P levels are quite small ($\delta \approx -0.012$ and $\delta \approx 0.07$, respectively), so they are nearly degenerate with higher orbital-angular-momentum levels. As the coupling energy of the excited electron with the electric field scales as n^2 and the contribution of the quantum defect to the level energy as n^{-3} at relatively modest field strengths isolated (low-l) levels may be considered degenerate with all higher-angular-momentum levels for high values of n and the linear Stark effect may easily be observed. Although the resemblance of helium and hydrogen Stark manifolds is striking the influence of levels having nonzero quantum defect is still present. In helium, contrary to the hydrogen case, noncrossing phenomena[16] between levels of adjacent manifolds are readily observable.

Results of several experiments on angular-momentum manifolds and avoided level crossings have been published (e.g., see Refs. 16 and 17), most of them related to the one-electron alkaline-metal elements. Those experiments were performed in low resolution (1–3 GHz) using pulsed-laser systems in contrast with the present experiment on helium with a cw laser (1-MHz resolution). In addition the excitation with narrow-band cw-laser radiation facilitates the study of the distribution of excitation strength over the different-momentum-manifold levels.

In Sec. II of this paper the theoretical background of the linear Stark effect is summarized and calculational procedures are presented. In Sec. III the experimental setup is briefly described whereas in Sec. IV the experimental results are discussed and analyzed. Conclusions are given in Sec. V.

 ©1989 The American Physical Society

II. THEORETICAL BACKGROUND

The Hamiltonian describing the interaction of the atom with a uniform electric field F directed along the z axis is

$$H_F = -\mathbf{P}\cdot\mathbf{F} = ezF \ , \tag{1}$$

where $\mathbf{P}$ is the electric-dipole operator. Stark spectra of helium Rydberg levels are calculated by diagonalizing the complete energy matrix in a spherical base in the presence of an electric field following the method of Zimmerman.[17] The diagonal elements of this energy matrix are the zero-field energies whereas the off-diagonal elements contain the electric field contribution. The zero-field energies for helium $W^0_{n,l}$ are calculated with the Rydberg formula with known quantum defects $\delta_{n,l}$,

$$W^0_{n,l} = I - \frac{R}{(n-\delta_{n,l})^2} \ . \tag{2}$$

I is the ionization limit and R the Rydberg constant. In helium $I = 198\,310.7723$ cm^{-1} and $R = 109\,772.2731$ cm^{-1}. Quantum defects for n around 40 and l up to 7 are given in Table I. These quantum defects were calculated with the explicit Rydberg-Ritz formula using the appropriate energy dependence derived from quantum defects up to $n=8$.[11] Quantum defects for $l>7$ are assumed to be zero.

The fine structure in the ^3P Rydberg levels of ^{4}He for n around 40 is smaller than 1 MHz and consequently may be neglected. In this case a purely LS-coupled base may be used[18] and the off-diagonal matrix element representing the Stark effect can be expressed in such a base. A general matrix element may then be written as

$$\langle n_1' l_1' n_2' l_2' L' S' M_L' M_S' | \mathbf{P}\cdot\mathbf{F} | n_1 l_1 n_2 l_2 L S M_L M_s \rangle = (-1)^{2L-M_L+l_1+l_2'+1} \begin{pmatrix} L & 1 & L' \\ -M_L & 0 & M_L' \end{pmatrix} \begin{Bmatrix} l_2 & L & l_1 \\ L' & l_2' & 1 \end{Bmatrix} \sqrt{(2L+1)(2L'+1)}$$
$$\times (-1)^{(l_{2_{\max}}-l_2'+1)/2} \sqrt{l_{2_{\max}}}\, eF R^{n_2 l_2}_{n_2' l_2'} \delta(M_S', M_S)\delta(S', S) \tag{3}$$

for $l_2' = l_2 \pm 1$ and zero otherwise. $l_{2_{\max}}$ is the largest of l_2 and l_2'. Here it is assumed that the electric field only acts on the Rydberg electron.

The transition integral $R^{nl}_{n'l'}$ can be expressed in single-electron radial wave functions $R_{nl}(r)$ as follows:

$$R^{nl}_{n'l'} = \int_0^\infty R_{n'l'}(r) r R_{nl}(r) r^2 dr \ . \tag{4}$$

To calculate this integral the method proposed by Zimmerman[17] using the Coulomb approximation of Bates and Damgaard[19] was applied.

There is no selection rule for n in Eq. (3) so, in principle, all n are dipole coupled by the electric field. However, the coupling between adjacent principal quantum numbers is relatively small compared to the dipole coupling within n due to smaller transition integrals [Eq. (4)]. Consequently it will depend on the value of the field strength how many n values must be taken into account to reproduce level positions accurately. For example, to calculate the (anti-) crossing between two levels of adjacent n manifolds at least these two n values should be used in the calculation.

To reproduce the relative intensities of the manifold peaks it is necessary to calculate the transition probability to excite a Stark state from a low-lying state. The oscillator strength for a transition from a ground state W, L, M_L to a Stark state W', M' is[20]

$$f_{W,W'} = \tfrac{2}{3}(W - W') \times \left| \sum_{W''} \sum_{L''} U^{W'}_{W'',L''}(F) \langle WLM_L | P | W''L''M' \rangle \right|^2 , \tag{5}$$

where $U^{W'}_{W'',L''}$ is the unitary transformation which diagonalizes the Stark matrix.

In the discussion of Stark manifolds it is more convenient to adapt quantum numbers used for the hydrogen

TABLE I. Quantum defects of ^{4}He $1snl$ levels from Martin (Ref. 11).

		n				
l	State	38	39	40	41	42
0	^1S	0.139 738	0.139 737	0.139 736	0.139 735	0.139 734
0	^3S	0.296 682	0.296 680	0.296 679	0.296 678	0.296 677
1	^1P	−0.012 138	−0.012 138	−0.012 138	−0.012 139	−0.012 139
1	^3P	0.068 346	0.068 347	0.068 347	0.068 348	0.068 348
2	^1D	0.002 110	0.002 110	0.002 111	0.002 111	0.002 111
2	^3D	0.002 886	0.002 886	0.002 886	0.002 887	0.002 887
3	F	0.000 438	0.000 438	0.000 438	0.000 438	0.000 438
4	G	0.000 125	0.000 125	0.000 125	0.000 125	0.000 125
5	H	0.000 048	0.000 048	0.000 048	0.000 048	0.000 048
6	I	0.000 017	0.000 017	0.000 017	0.000 017	0.000 017
7	K	0.000 008	0.000 008	0.000 008	0.000 008	0.000 008

case,[21] i.e., parabolic quantum numbers. Each component of the Stark manifold then corresponds to a Stark state $|nkm\rangle$, with $k=n_1-n_2$ in terms of the usual parabolic quantum numbers n_1 and n_2. These quantum numbers are related by $n=n_1+n_2+|m|+1$, so for fixed n and m, k ranges over the values $[n-|m|-1, n-|m|-3, \ldots, -n+|m|+1]$. Furthermore, the parabolic magnetic quantum number m is equal to M_L. It appears as if the parabolic representation provides a better base for calculating Stark manifolds. However, in the parabolic base the zero-field states are not diagonal as in the spherical case. Also, because of deviations from the hydrogenic case (quantum defects) the Stark states $|nkm\rangle$ are not pure; therefore, the Stark effect is not diagonal in the parabolic base. Thus most of the advantage using the parabolic representation is lost. Since it is more convenient to calculate manifold intensity profiles originating from a low-l-valued nondegenerate level [Eq. (5)] in the spherical base, this one is used in the diagonalization procedure.

As levels with different l values are not degenerate at zero-field, interesting, nonhydrogenic phenomena may appear in the observation of manifolds. This paper focuses on avoided crossings between Stark states of different n due to higher-order Stark effects. The repulsive interaction between the states originates from core interactions at zero field. These interactions, in fact, are represented by the quantum defects (Table I). Komarov *et al.*[22] have derived an explicit analytical formula to estimate the minimum separation W_0 between two Stark states from zero-field data,

$$\tfrac{1}{2}W_0=(nn')^{-3/2}\sum_{l\geq|m|}^{n_{\min}-1}(2l+1)\begin{pmatrix}(n-1)/2 & (n-1)/2 & l\\ (m+k)/2 & (m-k)/2 & -m\end{pmatrix}\begin{pmatrix}(n'-1)/2 & (n'-1)/2) & l\\ (m+k')/2 & (m-k')/2 & m\end{pmatrix}\delta_l\,. \tag{6}$$

The $3j$ symbols relate the zero-field data in spherical base with the Stark levels represented in the parabolic base.

III. EXPERIMENTAL SETUP

A detailed description of the experimental setup (Fig. 1) is presented elsewhere.[1] For this reason only a brief description, emphasizing details relevant for the present experiment, is given here.

Metastable states of helium were produced by running a discharge between a skimmer and a tantalum needle inserted in a quartz tube. The helium gas flow expanded through the nozzle of this quartz tube via the skimmer into the interaction region. Metastable state production was estimated to be in the order of 10^{14} atoms per second per steradian with a thermal velocity of 2000 m/s.[23] Experimental data showed that in the interaction region the ratio of the population of $1s2s\ ^1S_0$ versus $^3S_1$ metastable states is about 3. Doppler effects were reduced using a small nozzle orifice (0.2-mm diameter) and an adjustable collimating slit (0.3 mm, collimation ratio 1:600). The metastable beam was perpendicularly intersected with focused laser light. The interaction took place between two capacitor plates shielded in a metal box. The separation between the plates was measured to be 5.80(5) mm. The residual Doppler width of a field-free transition to a $1snp$ Rydberg level was about 10 MHz. The excited Rydberg atoms leaving the box were field ionized by applying a positive voltage of about 50 V to the box. The produced ions were accelerated into a quadrupole mass filter and the selected ^{4}He ions counted with an electron multiplier. The signal was stored on a minicomputer also controlling the laser scan. Furthermore part of the (visible) output of the dye laser was sent through a length-stabilized étalon (free spectral range of 148.9568 MHz). The Fabry-Pérot signal was also stored on the minicomputer for calibration purposes.

The ionization limit of ^{4}He is at about 25 eV while the metastable states lie around 20 eV. High Rydberg states may be excited from these metastable states with uv laser light. This was produced by intracavity frequency-doubling a cw ring dye laser (Spectra Physics 380D) using temperature-tuned nonlinear crystals.[3] To excite $1snp\ ^1P$ from $1s2s\ ^1S_0$ ($n\approx40$) laser light around 313 nm was produced using Rhodamine B dye and a rubidium dihydrogen phosphate (RDP) crystal. The transition $1s2s\ ^3S_1 \rightarrow 1snp\ ^3P$ is made with laser light around 260 nm using the dye coumarine 6 and a potassium dihydrogen phosphate (KDP) crystal. uv output was about 4 mW with 5-W pump power from an Ar^+ laser. The dye lasers were frequency stabilized, yielding bandwidths in the order of 1 MHz in the ultraviolet region. uv scans up to 75 GHz were made.

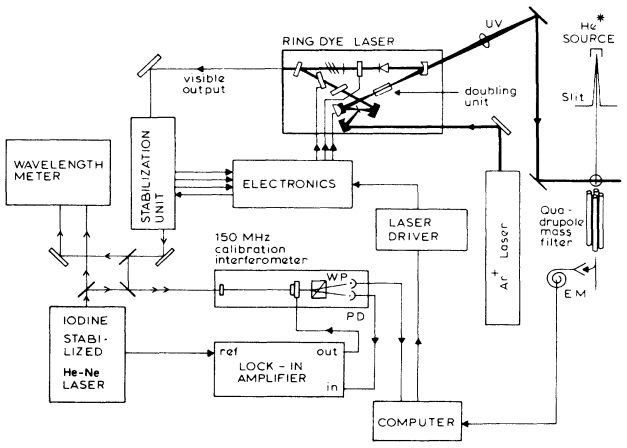

FIG. 1. Schematic of the experimental setup: EM, electron multiplier; WP, Wollaston prism; PD, photodiode.

IV. RESULTS AND DISCUSSION

Manifolds originating from excitations of ^1P as well as ^3P levels were studied. The only difference between singlet and triplet for high Rydberg states of helium is their quantum defect (see Table I) as the fine-structure splitting in the triplet states for high n may be neglected. Therefore, singlet and triplet manifolds are expected to show analogous behavior as a function of the field strength. Since the singlet manifolds are more pronounced than triplet manifolds due to higher population of the singlet metastable state this singlet case will be emphasized in the discussion. The polarization of the uv laser light was parallel to the electric field axis (π excitation). Starting from an S state together with the selection rule for an electric-dipole transition [$3j$ symbol in Eq. (3)] only $m=0$ manifolds may be excited.

A. "Isolated" manifolds

An example of a singlet angular-momentum manifold for $n=40$ and a field strength of 10.02 V/cm is shown in Fig. 2. The total width of the recorded spectrum is 60 GHz. The distance between the outermost peak at the high-frequency side of the $n=40$ manifold and the nearest peak of the $n=41$ manifold is 40 GHz, so the manifolds are still well separated. This manifold shows some characteristic features: strong signals at the low-frequency side, a steep fall in intensity with increasing frequency of the laser obviously resulting in suppression of manifold components and a reappearance of (weaker) signals at the high-frequency side. This behavior is typical for the $m=0$ manifolds of helium excited via singlet P states and strongly deviates from the pattern observed in the manifolds originating from $6sng\ ^1G_4$ levels in barium.[9] The strong signal at the low-frequency side in Fig. 2 is connected to the excitation of the $40\,^1S$ state ($\delta=0.14$, see Table I). This state is directly dipole coupled to the P state resulting in a large excitation probability. The singlet-P state with its negative quantum defect is originally located at the high-frequency side of the manifold. Obviously the outermost levels "absorb" most of the oscillator strength at the cost of Stark states in the middle of the manifold. Experimentally Stark states with parabolic quantum number k between -39 and -25 and between -3 and 39 were observed in the case shown in Fig. 2.

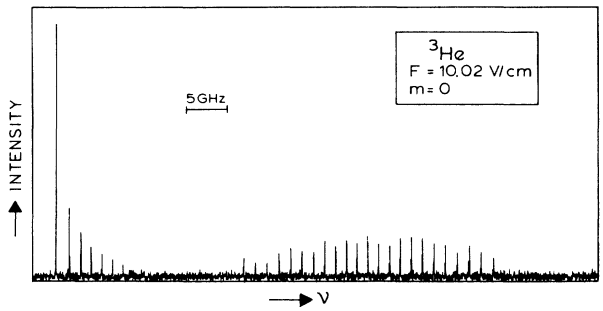

FIG. 2. Stark manifold at $F=10.02$ V/cm originating from the transition $1s2s\ ^1S_0 \rightarrow 1s40p\ ^1P$ in ^{4}He.

To compare experimental results with theoretical calculations some data adapation was necessary as not all manifold peaks had the same Doppler limited linewidth (10 MHz). Broadening due to field inhomogeneities was present. As in first-order perturbation theory the energy of the hydrogenic Stark levels is proportional to $\frac{3}{2}nkF$ (Ref. 21) a field inhomogeneity ΔF will mostly affect the outermost levels of the manifold with largest k values. From the observed linewidth variation an inhomogeneity of 5 mV/cm was deduced. For this reason the peak intensity was taken to be the integrated signal strength concentrated in the center of the resonance. The thus obtained results are derived from the spectrum in Fig. 2 are given in Fig. 3 where also the manifold pattern calculated with the diagonalization procedure outlined in Sec. II is included. To reproduce level positions to within the experimental accuracy at the MHz level it turned out to be necessary to include three n values ($n=39$, 40, and 41) in the diagonalization. The overall agreement between experiment and calculation is good. For example, the intensity minimum in the middle of the manifold is reproduced. From a comparison of calculated values and observations it follows that the levels with k in between -25 and -3 indeed were too weak to be observable. It appears as if the calculated intensities at the low-frequency side are slightly underestimated and at the high-frequency side overestimated compared to experiment. However, the calculation was based on constant laser power, which, in fact, was not the case for the large laser scans necessary to record the spectra. Experimentally the laser power varied between 4.5 mW at the low-frequency side and 3.5 mW at the high-frequency side in the case shown in Figs. 2 and 3.

Apart from the intensity distribution the triplet manifold shows the same behavior as the singlet case. The intensity distribution in the triplet case is different as here the regular ordering of levels (^3S state below ^3P state below higher l states, see Table I) holds.

B. Avoided crossings

1. *Avoided crossings of two levels of adjacent manifolds*

With increasing strength of the field the gap between adjacent manifolds diminishes as shown in the spectra of

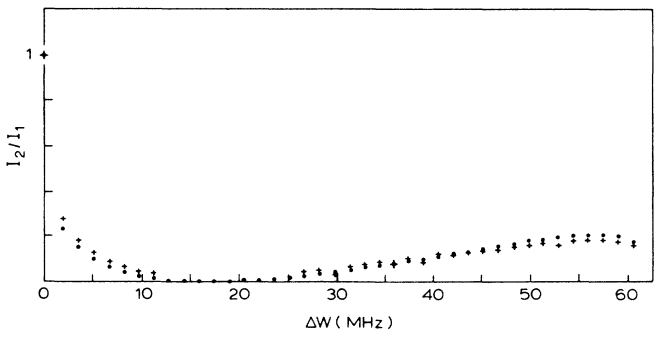

FIG. 3. Experimental (+) and calculated (●) relative intensities as a function of energy for the Stark manifold at $F=10.02$ V/cm as shown in Fig. 2.

Fig. 4 for $n=40$ and 41, again obtained in excitation from the singlet metastable state. Unlike the hydrogen case the levels do not cross with increasing field. An example is given in Fig. 5 for the two outermost levels of the $n=41$ ($|41,-40,0\rangle$) and $n=40$ ($|40,39,0\rangle$) manifolds for electric fields between 16 and 16.5 V/cm. The origin of this typical avoided crossing is the nondegeneracy at zero field of levels with different values of l, contrary to the hydrogen case. Especially the S states have significant quantum defects resulting in a coupling of, e.g., the $(n+1)s$ state both with the $(n+1)p$ and np states in the presence of the field. In sum then there are dipole couplings between manifolds originating from different n and consequently Stark manifolds with different n values cannot be treated as being independent as in the case of hydrogen.

In Fig. 6 the experimental energy-level separation ΔW is plotted as a function of field strength in the region of the avoided crossing of Fig. 5. Also included are the results of a calculation using the diagonalization method. To obtain good agreement between experiment and calculations in the crossing region at least four n values ($n=39$, 40, 41, and 42) had to be incorporated in the diagonalization. In Table II experimental and calculated values for the minimum separation W_0 in the avoided crossing $|41,-40,0,\rangle\leftrightarrow|40,39,0\rangle$ both for the singlet and triplet manifolds are given.

According to the discussion of avoided crossings in

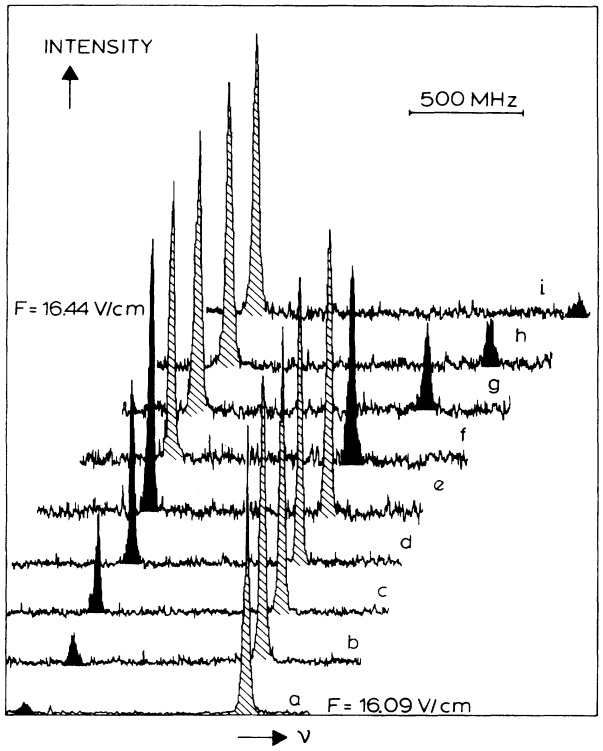

FIG. 5. Experimental map of the avoided crossing of the ^{4}He manifold levels $|40,39,0\rangle\leftrightarrow|41,-40,0\rangle$.

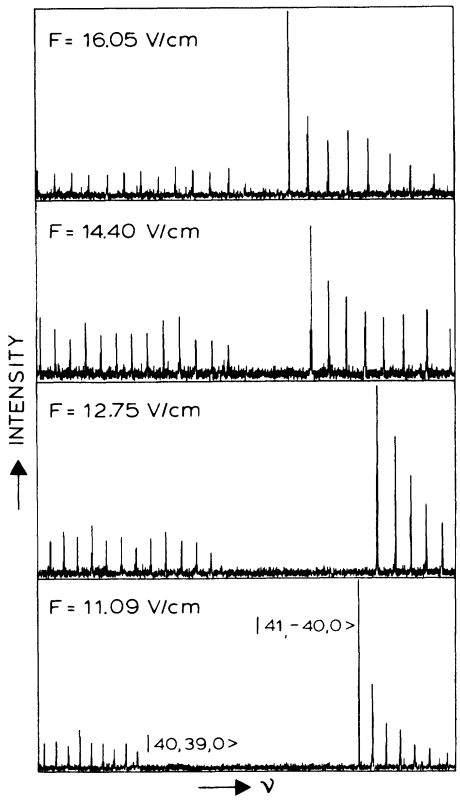

FIG. 4. $n=40$ (low-frequency side) and $n=41$ (high-frequency side) manifold in ^{4}He with increasing field strength.

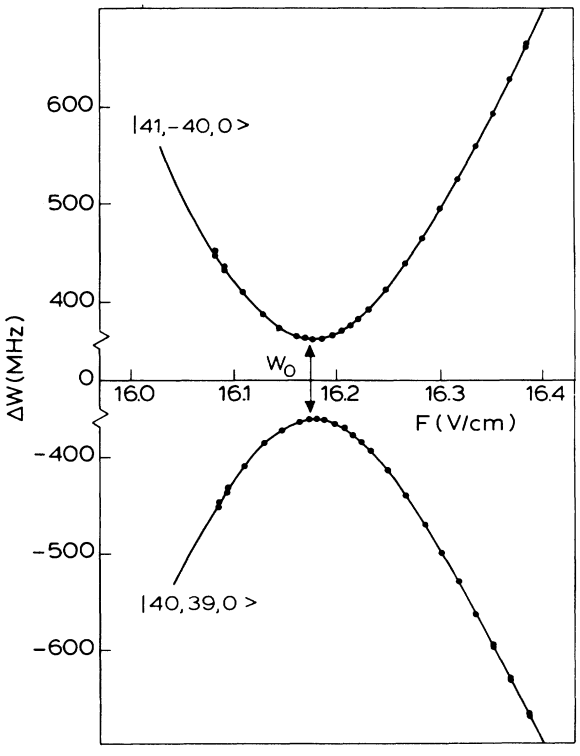

FIG. 6. Avoided crossing $|40,39,0\rangle\leftrightarrow|41,-40,0\rangle$ in ^{4}He. Dots, experimental; curve, calculated.

TABLE II. Experimental and calculated values of the minimum separation W_0 in the avoided crossing of the ^{4}He manifold levels $|40,39,0\rangle \leftrightarrow |41,-40,0\rangle$ (in MHz). The fit of the avoided-level-crossing results in an uncertainty of 3 MHz in W_0.

	Singlet	Triplet
Experimental	720(3)	586(3)
Calculated	721.4	588.9
F (V/cm)	16.18	15.58

Sec. II W_0 is expected to be larger with increasing deviation from a hydrogenic state and will be maximal when an isolated state is positioned halfway in between two manifolds, i.e., when its quantum defect is 0.5. From Table I it follows that $\delta(^3S) \approx 2\delta(^1S)$. However, $W_0(^3S)$ is not larger than $W_0(^1S)$ but even smaller. A possible reason is that for the avoided crossing in the triplet case the $41\,^3S$ state ($|41,-40,0\rangle$) has not yet completely merged with the $n=41$ manifold. So there is a larger separation between this state and the neighboring $|41,-38,0\rangle$ Stark state than between the other Stark states in this manifold. This will result in a smaller energy gap W_0 between this orginally ^3S state and the Stark state $|40,39,0\rangle$.

Using relation (6) to calculate W_0 a value of 573.6 MHz is obtained for the singlet case, 146 MHz below the experimental value. This difference originates from the fact that in the model of Komarov *et al.*[22] only two adjacent n values are considered, which is obviously not sufficient as follows from the diagonalization procedure. Furthermore the description of Komarov *et al.* is based upon the assumption that avoided crossings between Stark states occur in the hydrogenic or linear Stark effect regime. This is obviously not correct for the avoided crossing in the triplet case as the ^3S state has not yet completely merged with the manifold (and may only be tentatively be assigned with parabolic quantum numbers $|41,-40,0\rangle$). A calculation of W_0 in this case yields a value of 2424 MHz, even further off from the experimental value (Table II) than in the singlet case. Inspection of the model of Komarov *et al.* shows that Eq. (6) basically contains the transformation from spherical to parabolic coordinates. The most elaborate way of calculating W_0 will be to derive the appropriate F-dependent frame transformation between actual Stark states (in parabolic base) and the zero-field states (in spherical base). In fact, such a frame transformation is the issue of the (multi)channel quantum-defect theory [(M)QDT] of the Stark effect.[24,25]

Also, a value of the minimum energy separation between the Stark states $|50,-49,0\rangle$ and $|49,48,0\rangle$ in the triplet case was determined (286 MHz). According to Zimmerman[17] the minimum crossing gap W_0 roughly scales as n^{-4} as the density of Stark states for $m=0$ is proportional to n^4. The ratio of the observed triplet gaps is 0.49, in reasonable agreement with the scaling-law ratio of 0.45.

Finally the mixing of wave functions and the resulting relative peak intensities in the avoided crossing region were also calculated. In general, the experimental intensities could be reproduced although the comparison was not straightforward due to scatter in the observed signal strength.

2. *Threefold avoided crossings*

In Sec. IV B 1 the merging of two levels of adjacent manifolds was discussed. Also more complicated anticrossing phenomena could be observed. An example is given in Fig. 7 where at a field strength of about 34 V/cm the two outermost levels of the $n=41$ and 39 manifold ($|41,-40,0\rangle$ and $|39,38,0\rangle$, respectively) and the $|40,-3,0\rangle$ level of the $n=40$ manifold show a complicated avoided-crossing pattern. When the even k states are far apart the level $k=-3$ of the $n=40$ manifold is not observable as it is located in the low-intensity part (see Figs. 2 and 3). With decreasing separation the $|40,-3,0\rangle$ signal gains intensity at the cost of the outer two signals. For certain values of the field the outermost peaks completely vanish while the middle one has maximum intensity and shows a narrow linewidth (10 MHz).

In Fig. 8 the experimental energy-level separations in the region of this crossing pattern are displayed as a function of F. Energy separations of the two outermost levels are plotted relative to the $|40,-3,0\rangle$ level, which falls on the abscissa of Fig. 8. In the plot four energy extrema W_1-W_4 in the crossing region may be recognized, values of which are collected in Table III. To reproduce the

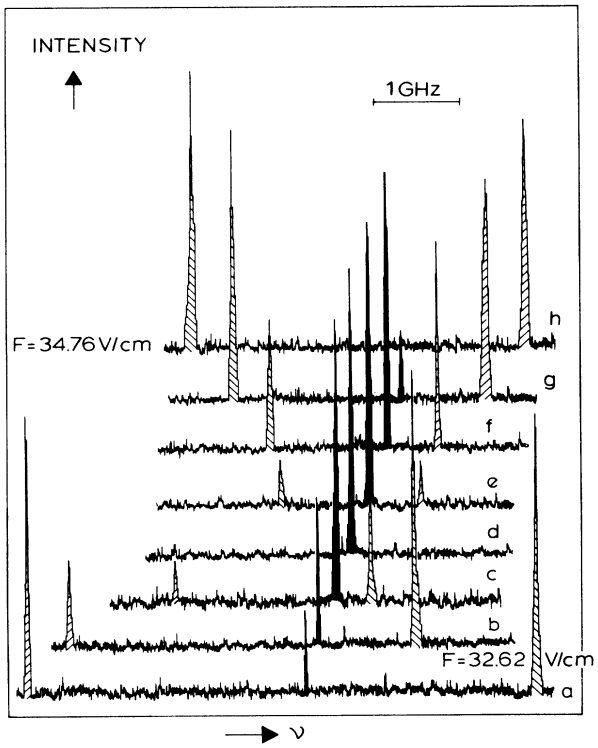

FIG. 7. Experimental map of the threefold avoided crossing of the manifold levels $|39,38,0\rangle \leftrightarrow |40,-3,0\rangle \leftrightarrow |41,-40,0\rangle$ in ^{4}He.

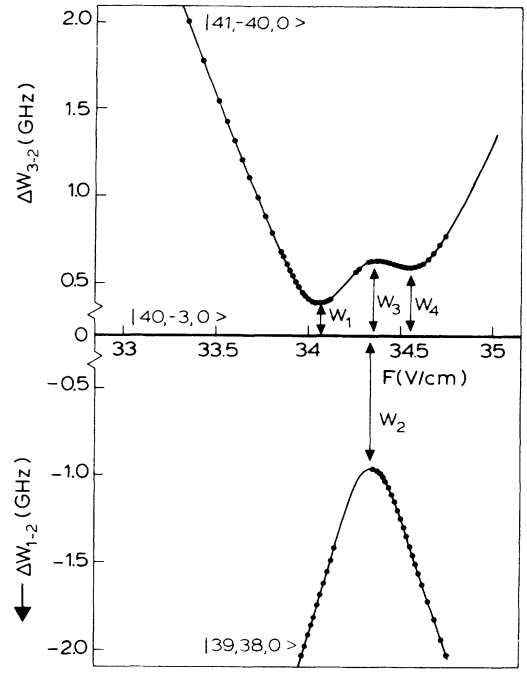

FIG. 8. Avoided crossing $|39,38,0\rangle \leftrightarrow |40,-3,0\rangle \leftrightarrow |41,-40,0\rangle$ in ^{4}He. Dots, experimental; curve, calculated.

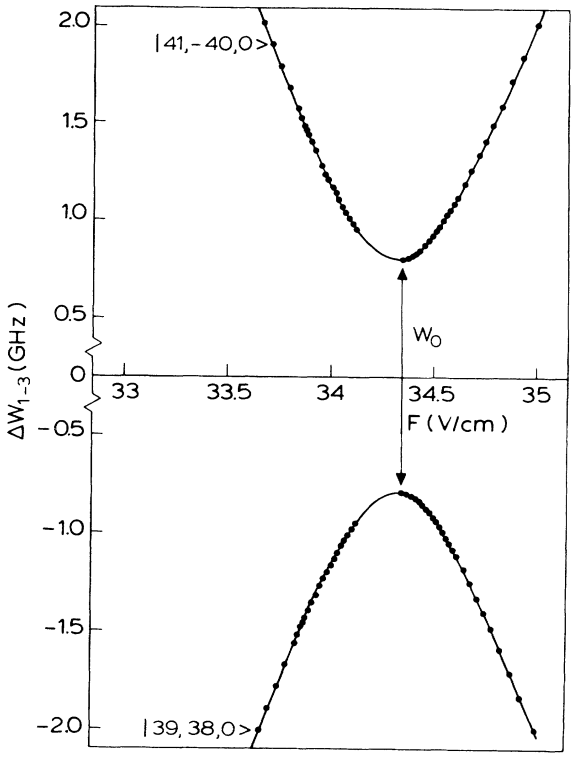

FIG. 9. Avoided crossing $|39,38,0\rangle \leftrightarrow |41,-40,0\rangle$ in ^{4}He. Dots, experimental; curve, calculated.

data shown in Fig. 8 and Table III at these relatively high values of the field strength a diagonalization of an even larger energy matrix including five n values ($n=38$, 39, 40, 41, and 42) was necessary. The results of this calculation are included in Table III and Fig. 8. In Fig. 9 the energy separation of the two outermost levels alone is plotted, showing the regular avoided-crossing pattern discussed in Sec. IV B 1 with a minimum separation $W_0 \approx |W_2| + |W_3| = 1587(3)$ MHz (experimental value) or 1588 (calculated value).

Figures 8 and 9 show that, starting at low F (30 V/cm), with increasing field strength the separation between the levels $|41,-40,0\rangle$ and $|39,38,0\rangle$ decreases as if the level $|40,-3,0\rangle$ is not present, up to some value (F around 34 V/cm) where its influence becomes apparent. Here the $|41,-40,0\rangle$ level is repelled by the $|40,-3,0\rangle$ level. This repulsion disappears again at $F=34.3$ V/cm where the repulsive interaction with the $|39,38,0\rangle$ level takes over. The limited influence of the $|40,-3,0\rangle$ level may be explained considering the signal strengths. The intensity observed is a direct measure of the P character mixed into the wave functions of the Stark states. It is now obvious that when the $|41,-40,0\rangle$ and $|39,38,0\rangle$ levels are far apart [see Figs. 7(a) and 7(h)] only their mutual interaction is important. As the $|40,-3,0\rangle$ level in the middle has no excitation strength coupling with the outermost levels is not noticeable. With increasing F the $|40,-3,0\rangle$ level gains signal strength up to some value ($F=34.05$ V/cm) where its intensity (I_2) becomes the sum of the intensities of the outermost peaks ($I_2 = I_1 + I_3$ both theoretically and experimentally). The corresponding increase of P character in the $|40,-3,0\rangle$ wave function thus results in interaction with the outermost levels. At $F=34.55$ V/cm the intensity of the $|40,-3,0\rangle$ excitation again is the sum of intensities of the other two peaks after a decrease in between. At still higher fields $|40,-3,0\rangle$ vanishes from the spectrum and its influence again is negligible.

C. Remarks

From the discussion of isolated angular-momentum manifolds and avoided crossings in the n-mixing regime in Secs. IV A and IV B it follows that with increasing F

TABLE III. Experimental and calculated values of extrema W in the threefold avoided crossing of the ^{4}He manifold levels $|39,38,0\rangle \leftrightarrow |40,-3,0\rangle \leftrightarrow |41,-40,0\rangle$ (in MHz). The fit of the threefold avoided-level-crossing results in an uncertainty of 3 MHz in the extrema W.

	W_0	W_1	W_2	W_3	W_4
Experimental	1587(3)	383(3)	−960(3)	627(3)	582(3)
Calculated	1588	385.5	−963	630	585

more and more n values must be included in the diagonalization of the energy matrix to reproduce the highly accurate data. This puts high demands on the numerical methods and will ultimately limit the applicability of this diagonalization procedure. In the case of the threefold avoided crossing discussed in Sec. IV B 2, e.g., five n values had to be considered, resulting in the diagonalization of a 200×200 energy matrix. At even higher field strengths other physical processes become important. In the presence of the field the ionization limit is lowered yielding an increased tunneling probability. The influence of the continuum is not accounted for using the diagonalization method.

In this case the alternative approach as proposed by Harmin[24] where the Stark effect is incorporated in the framework of quantum-defect theory, may be applied. However, in this theory large energy matrices also have to be dealt with. Again the avoided crossings will be a sensitive tool to test the theory for both weak and strong electric fields.

V. CONCLUSIONS

The development of an efficient helium metastable beam source enabled the investigation of high $1snp$ Rydberg states with cw laser light in the presence of an electric field. As these P states have almost zero quantum defect already at modest electric field strengths transitions from quadratic to linear Stark effect (angular-momentum manifold) may be observed. However, states with nonzero quantum defect (especially the S state coupled to the P state by the field) causes the atom not to act purely hydrogenic. In the electric field states of different n are also dipole-coupled and n mixing occurs. This gives rise to avoided crossings when different Stark states approach each other. These phenomena were studied for triplet as well as singlet states for n around 40 and $m=0$. As might be expected these avoided crossings are a sensitive probe for the mixing different Stark states $|nkm\rangle$. This also puts high demands on the calculational method. In this work the method of diagonalization of the complete energy matrix was applied including up to five n values. A straightforward approach of relating avoided crossings between two levels of adjacent manifolds with zero-field data failed, making clear that these phenomena in helium cannot be described accurately with a two-level model. This was confirmed by the diagonalization calculation where four n values ($n=39-42$) were needed to reproduce the avoided crossing $|41,-40,0\rangle\leftrightarrow|40,39,0\rangle$ and five ($n=38-42$) to calculate the threefold avoided crossing $|41,-40,0\rangle\leftrightarrow|40,-3,0\rangle\leftrightarrow|39,38,0\rangle$ accurately within the experimental error (3 MHz). However, for higher field strengths this method will not hold because of, i.e., the influence of the continuum. An alternative approach is quantum-defect theory incorporating the Stark effect. Also for this theory the avoided crossings will be a sensitive test. This is planned to be a subject of future study in our laboratory.

ACKNOWLEDGMENTS

The authors would like to thank Wim Vassen, Tony van der Veldt, and Jacques Bouma for their support with the experiments. Financial support from the Foundation for Fundamental Research on Matter (FOM) and the Netherlands Organization for the Advancement of Research (NWO) is gratefully acknowledged.

[1]W. Vassen and W. Hogervorst, Phys. Rev. A (to be published).
[2]W. Vassen, Ph.D. thesis, Vrije Universiteit, Amsterdam, Holland, 1988.
[3]E. Eliel, Ph.D. thesis, Vrije Universiteit, Amsterdam, Holland, 1982.
[4]B. H. Post, Ph.D. thesis, Vrije Universiteit, Amsterdam, Holland, 1985.
[5]E.A.J.M. Bente and W. Hogervorst, Phys. Rev. A **36**, 4081 (1987).
[6]U. Fano and A.R.P. Rau, *Atomic Collisions and Spectra* (Academic, New York, 1986).
[7]M. Aymar, Phys. Rep. **110**, 163 (1984).
[8]K. A. H. van Leeuwen, Ph.D. thesis, Vrije Universiteit, Amsterdam, Holland, 1984.
[9]C. T. W. Lahaye, W. Hogervorst, and W. Vassen, Z. Phys. D **7**, 37 (1987).
[10]G. W. F. Drake, Nucl. Instrum. Methods **31**, 7 (1988).
[11]W. C. Martin, Phys. Rev. A **36**, 3575 (1987).
[12]W. Schilling, Y. Kriescher, A. S. Aynacioglu, and G. von Oppen, Phys. Rev. Lett. **59**, 876 (1987).
[13]G. G. Tepehan, H-J. Beyer, and H. Kleinpoppen, J. Phys. B **18**, 1125 (1985).
[14]W-D. Perschamann, G. von Oppen, and D. Szostak, Z. Phys. A **311**, 49 (1983).
[15]A. S. Aynacioglu, G. von Oppen, W-D. Perschmann, and D. Szostak, Z. Phys. A **303**, 97 (1981).
[16]J. R. Rubbmark, M. M. Kash, M. G. Littman, and D. Kleppner, Phys. Rev. A **23**, 3107 (1981).
[17]M. L. Zimmerman, M. G. Littman, M. M. Kash, and D. Kleppner, Phys. Rev. A **20**, 2251 (1979).
[18]E. S. Chang, Phys. Rev. A **35**, 2777 (1987).
[19]D. R. Bates and A. Damgaard, Philos. Trans. R. Soc. London, **242**, 101 (1949).
[20]R. D. Cowan, *The Theory of Atomic Structure and Spectra* (University of California, Berkeley, 1981).
[21]H. A. Bethe and E. E. Salpeter, *Quantum Mechanics of One- and Two-electron Atoms* (Springer, Berlin, 1957).
[22]I. V. Komarov, T. P. Grozdanov, and R. K. Janev, J. Phys. B **13**, L573 (1980).
[23]D. W. Fahey, W. F. Parks, and L. D. Schearer, J. Phys. E **13**, 381 (1980).
[24]D. A. Harmin, Phys. Rev. A **26**, 2656 (1982).
[25]K. Sakimoto, J. Phys. B **19**, 3011 (1986).